



# Contribution to the crystal chemistry of lead-antimony sulfosalts: systematic Pb-versus-Sb crossed substitution in the plagionite homologous series,



Yves Moëlo<sup>1</sup> and Cristian Biagioni<sup>2</sup>

<sup>1</sup>Institut des Matériaux Jean Rouxel (IMN) – UMR 6502, Université de Nantes, CNRS, 44000 Nantes, France

<sup>2</sup>Dipartimento di Scienze della Terra, Università di Pisa, Via S. Maria 53, 56126 Pisa, Italy

**Correspondence:** Yves Moëlo (yves.moelo@cnr-immn.fr)

Received: 5 July 2020 – Revised: 1 October 2020 – Accepted: 16 October 2020 – Published: 14 November 2020

**Abstract.** The plagionite homologous series contains four well-defined members with the general formula  $\text{Pb}_{1+2N}\text{Sb}_8\text{S}_{13+2N}$ : fülöppite ( $N = 1$ ), plagionite ( $N = 2$ ), heteromorphite ( $N = 3$ ), and semseyite ( $N = 4$ ). The crystal structure of several natural and synthetic samples of fülöppite, plagionite, and semseyite have been refined through single-crystal X-ray diffraction, confirming the systematic Pb-versus-Sb crossed substitution observed previously in semseyite and fülöppite. This crossed substitution takes place mainly in two adjacent cation sites in the middle of the constitutive SnS-type layer. The substitution coefficient  $x$  appears variable, even for a given species, with the highest values observed in synthetic fülöppite samples. The developed structural formula of the plagionite homologues can be given as  $\text{Pb}_{2N-1}(\text{Pb}_{1-x}\text{Sb}_x)_2(\text{Sb}_{1-x}\text{Pb}_x)_2\text{Sb}_6\text{S}_{13+2N}$ . In the studied samples,  $x$  varies between  $\sim 0.10$  and  $0.40$ . In the ribbons within the SnS-type layer, (Pb/Sb) mixing can be considered the result of the combination, in a variable ratio, of two cation sequences, i.e. (Sb–Sb–Sb)–Pb–Sb–(…), major in plagionite and semseyite, and (Sb–Sb–Sb)–Sb–Pb–(…), major in fülöppite and, probably, in heteromorphite. The published crystal structure of synthetic “Pb-free fülöppite” is revised according to this approach. It would correspond to a Na derivative, with a proposed structural formula of  $(\text{Na}_{0.5}\text{Sb}_{0.5})(\text{Na}_{0.2}\text{Sb}_{0.8})_2(\text{Na}_{0.3}\text{Sb}_{0.7})_2\text{Sb}_6\text{S}_{15}$ , ideally  $\text{Na}_{1.5}\text{Sb}_{9.5}\text{S}_{15}$ . In fülöppite, increasing  $x$  induces a flattening of the unit cell along  $c$ , with a slight volume decrease. Such a general Pb-versus-Sb crossed substitution would attenuate steric distortions in the middle of the SnS-type layer of the plagionite homologous series. Crystallization kinetics seem the main physical factor that controls such an isochemical substitution.

**Dedicated to the memory of Dr. Nadejda N. Mozgova (1931–2019), Russian mineralogist of the Institute of Geology of Ore Deposits (IGEM Moscow), specialist of sulfosalts systematics.**

## 1 Introduction

Plagionite,  $\text{Pb}_5\text{Sb}_8\text{S}_{17}$ , defined by Rose (1833), is the chief member of one of the oldest groups of sulfosalts, along with fülöppite  $\text{Pb}_3\text{Sb}_8\text{S}_{15}$ , heteromorphite  $\text{Pb}_7\text{Sb}_8\text{S}_{19}$ , and semseyite  $\text{Pb}_9\text{Sb}_8\text{S}_{21}$ . On the basis of their crystal morphology, they were initially described as “tabular lead sulfosalts”, in

opposition to “acicular lead sulfosalts”, e.g. boulangerite, zinkenite, and jamesonite (Spencer, 1899). The comparison of parameter ratios through goniometric measurements led Spencer (1899) to the definition of a morphotropic series, a precursor concept of the modern definition of homologous series.

The crystal structures of these four members were resolved during the 1970s, i.e. plagionite from Wolfsberg, Germany (Cho and Wuensch, 1970, 1974); semseyite (Kohatsu and Wuensch, 1974a); fülöppite from Baia Mare (previously known as Nagybánya), Romania (Edenharter and Nowacki, 1974, 1975a; Nuffield, 1975); and heteromorphite

from Wolfsberg, Germany (Edenharter and Nowacki, 1975b; Edenharter, 1980). Swinnea et al. (1985) described the crystal structure of a synthetic Pb-free analogue of fülöppite (in fact a Na-substituted fülöppite derivative – see below).

A detailed crystal chemical analysis permitted Kohatsu and Wuensch (1974b) to develop a general structural scheme for this group. This study can be considered the basis for the modern definition of the plagionite homologous series,  $\text{Pb}_{1+2N}\text{Sb}_8\text{S}_{13+2N}$ , with the following members: fülöppite ( $N = 1$ ), plagionite ( $N = 2$ ), heteromorphite ( $N = 3$ ), and semseyite ( $N = 4$ ). Takéuchi (1997), as part of his general study of trochochemical cell twinning, gave considerable detail about the crystal chemistry of the plagionite series. Recently, Makovicky (2019) presented this series as an example of a homologous series among sulfosalts.

In nature, this series has very simple chemistry. Fluctuations in the Pb/Sb atomic ratio correspond to microscopic or submicroscopic lamellar syntactic intergrowths (Mozgova and Borodaev, 1972; Moëlo, 1983) visible in crossed polars in reflected light or with SEM imaging. Rarely, arsenic may substitute for antimony (up to  $\sim 10$  at. %–12 at. % in plagionite from Rujevac, former Yugoslavia; Janković et al., 1977; Moëlo et al., 1983). Other erratic minor components detected by electron microprobe analysis would correspond to impurities. Rayite,  $(\text{Ag,Tl})_2\text{Pb}_8\text{Sb}_8\text{S}_{21}$ , was defined as an (Ag,Tl)-rich derivative of semseyite (Basu et al., 1983) on the basis of its X-ray powder diffraction (XRPD) pattern, but this interpretation was later debated (Roy Choudury et al., 1989; Bente and Meier-Salimi, 1991), and crystal structure data are still lacking.

Re-examination of the original structural data for fülöppite (Nuffield, 1975) led Swinnea et al. (1985) to highlight minor Sb substitution in a Pb site, coupled with the reverse substitution of Pb in an adjacent Sb position. A similar Pb-versus-Sb crossed substitution was obtained on semseyite from Wolfsberg by Matsushita et al. (1997) and recently refined and detailed by Matsushita (2018).

During the systematic study of sulfosalt mineralogy in ore deposits of the Apuan Alps, a new occurrence of plagionite was identified in the baryte + pyrite + iron oxide deposit of the Monte Arsiccio mine (e.g. Costagliola et al., 1990). Its crystal structure study, together with those of other samples of plagionite (natural), fülöppite (natural and synthetic), and semseyite (natural) allowed confirmation that such a Pb/Sb crossed substitution is a general feature of members of the plagionite homologous series. Detailed results are presented here.

## 2 Modular description of crystal structures in the plagionite series

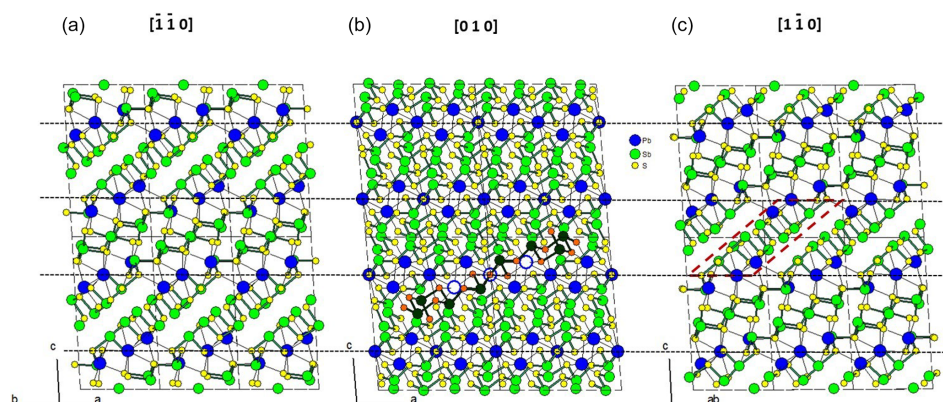
Modular analysis constitutes a powerful approach for the bottom-up description of complex crystal structures of lead sulfosalts, taking into account polyhedra connection ac-

ording to modules of increasing dimensionality: 0D (finite groups), 1D (chain, ribbon, column), 2D (slab, layer), and 3D (whole structure). Each module can be symbolized by its 3D polyhedra width. For instance, symbol  $2/3/\infty$  would correspond to a ribbon, two-polyhedra thick and three-polyhedra large.

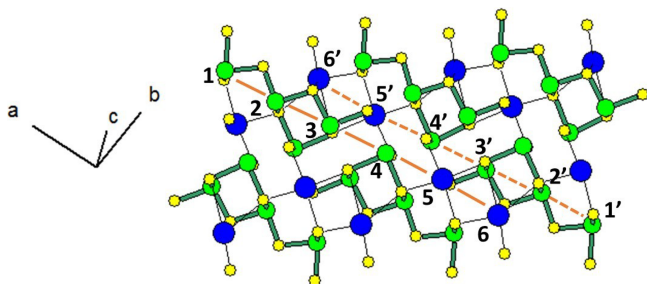
Application of modular analysis to the plagionite series permits five organization levels to be distinguished, from the bottom, i.e. polyhedra around metal or S atoms (level 1 – 3D symbol  $1/1/1$ ; see the example of the plagionite structure in Cho and Wuensch, 1974), up to the top, i.e. the whole structure (level 5 – dimensionality  $\infty/\infty/\infty$ ). Level 4 corresponds to a layered organization (Kohatsu and Wuensch, 1974b), with a single type of layer stacking along  $c$  with two orientations according to the binary axis. These layers correspond to diagonal slabs of the  $\text{SnS}$  archetype (Makovicky, 1989), with a distortion referring more exactly to the  $\text{TlSbS}_2$  archetype (Takéuchi, 1997; Matsushita, 2018). Layer width increases with the homologue number  $N$ , through the addition of Pb polyhedra, corresponding to the stacking of  $(4\text{ Sb} + N\text{ Pb})$  cations (dimensionality  $(4 + N)/\infty/\infty$ ). Layers are connected by an additional Pb atom.

Figure 1 represents the layered structure of fülöppite along  $b$  (Nuffield, 1975). Projection according to  $[\bar{1}\bar{1}0]$  or  $[1\bar{1}0]$  reveals ribbon stacking within each layer. Each ribbon is two atoms thick, six cations large (Fig. 1c – four Sb and two Pb, including the Pb atom at the margin – dimensionality  $2/6/\infty$ ). Projection of a single ribbon perpendicular to its flattening (see Fig. 1c) indicates oblique 2-atom-thick  $\times$  2-atom-thick rows (Fig. 2), with a finite length of six atoms (level 2 – dimensionality  $2/2/6$ ). In a row ( $[110]$  direction of PbS archetype), there are two cation sequences, Sb–Sb–Sb–Sb–Pb–Pb and its reverse one. Nevertheless, this approach at level 2 is incomplete. Due to the stereochemical activity of its lone electron pair, trivalent Sb shows a dissymmetric coordination, with three strong Sb–S bonds (i.e.  $\text{SbS}_3$  polyhedra with eccentric triangular pyramidal coordination). In the plagionite series,  $\text{SbS}_3$  polyhedra coalesce to form finite groups (polymers), which have been described in fülöppite and plagionite by Edenharter and Nowacki (1974) and in heteromorphite and semseyite by Edenharter (1980). These groups are represented in Fig. 3, along with neighbouring Pb atoms. They are symmetric across the layer boundary via 2-fold rotation (2-fold axis parallel to  $b$  – see projection along  $b$  in Fig. 1). Whereas in fülöppite, plagionite, and heteromorphite, all Sb sites are connected in an  $\text{Sb}_8\text{S}_m$  group (Fig. 3a–c), in semseyite there is an  $\text{Sb}_6\text{S}_{13}$  group with two isolated  $\text{SbS}_3$  polyhedra (Fig. 3d).

Plagionite, heteromorphite, and semseyite present the same cleavage plane according to  $\{112\}$ . It corresponds to the flattening of the ribbons according to  $(100)_{\text{PbS}}$ . It has not been observed up to now in fülöppite but ought to be present for the same structural reasons.



**Figure 1.** Crystal structure of fülöppite: projection along  $b$  (b),  $[1\bar{1}0]$  (a), and  $[1\bar{1}0]$  (c). An  $\text{Sb}_8\text{S}_{15}$  polymer across two layers has been represented (b – Sb: black circle; S: orange circle). In (c) a two-atom-thick ribbon has been delimited (lozenge; red tie line). Layering: black tie lines.



**Figure 2.** Projection of the SnS-type, two-atom-thick ribbon of the crystal structure of fülöppite, according to Nuffield (1975). Two symmetric oblique cation rows alternate (1 to 6, and 1' to 6'), with the sequence Sb–Sb–Sb–Sb–Pb–Pb. Short Sb–S bonds have been highlighted in green.

### 3 Experimental

#### 3.1 Studied samples

Eight natural and synthetic specimens were studied: fülöppite (3), pligionite (3), and semseyite (2).

##### 3.1.1 Fülöppite

Sample F1 is a crystal extracted from an old Romanian specimen from the Dealul Crucii deposit (Baia Mare district; La Sorbonne collection, Paris – now Jussieu collection). It occurs as millimetre-sized automorphic crystals on quartz.

Sample F2 is represented by well-developed synthetic crystals of  $\text{Pb}_3\text{Sb}_8\text{S}_{15}$  obtained by Mozgova et al. (1987) through a hydrothermal process ( $\text{PbS}:\text{Sb}_2\text{S}_3$  mixture, 1 mol/L  $\text{H}_2\text{SO}_4$ ; temperature gradient 270–300 °C; run duration 6 d). Some of them were given to one of us (Yves Moëlo) by Nadejda Mozgova.

Sample F3 is represented by rare crystals obtained as a by-product of a hydrothermal synthesis at 200 °C (3 weeks)

from a mixture of galena and stibnite, together with the addition of  $\text{PbCl}_2$  and  $\text{FeCl}_3$  (run XIV-1, duration 3 weeks; Moëlo, 1983). The main product was a chloro-sulfosalt (“Phase Y”,  $\sim \text{Pb}_{11}\text{Sb}_{10}\text{S}_{23}\text{Cl}_4$ ; Moëlo, 1979).

##### 3.1.2 Pligionite

Sample P1 is a new occurrence of pligionite discovered at the Monte Arsiccio mine (Apuan Alps, Tuscany, Italy), where this mineral occurs as compact masses or, rarely, as tabular crystals, showing growth features, up to 5 mm in size. Pligionite is associated with extremely thin acicular crystals, from black to reddish in colour, of TI-bearing chovanite, in fractures of metadolostone from the Sant’Olga level. Electron microprobe analysis of pligionite gave (mean of 15 spot analyses; wt %) Pb 40.40(34), Sb 38.09(22), S 21.37(11), and sum 99.85(52). On the basis of  $\text{Pb} + \text{Sb} = 13$  atoms per formula unit, the chemical formula of pligionite from Monte Arsiccio is  $\text{Pb}_{4.99(2)}\text{Sb}_{8.01(2)}\text{S}_{17.05(2)}$ , in agreement with the ideal formula  $\text{Pb}_5\text{Sb}_8\text{S}_{17}$ .

Sample P2 is a specimen from the well-known Wolfsberg antimony deposit, Germany (from an old French collection).

Sample P3 is represented by xenomorphic plurimillimetric crystals of pligionite in a siderite matrix collected in the dumps of the small Pb deposit of Saint-Georges-au-Puix near Lepuix (Giromagny district, south of the Vosges massif, Territoire de Belfort department, France; Fluck et al., 1975). Numerous Sb sulfosalts were observed in this quartz vein: boulangerite, semseyite, pligionite, zinkenite, fülöppite, berthierite, bournonite, tetrahedrite, and chalcostibite (Weil et al., 1975; Moëlo, 1983). Microprobe analysis of pligionite gave (wt %; mean of three spot analyses) Pb 40.32, Sb 38.47, S 21.25, and sum 100.04. Its formula unit is  $\text{Pb}_{4.96}\text{Sb}_{8.04}\text{S}_{16.92}$ .

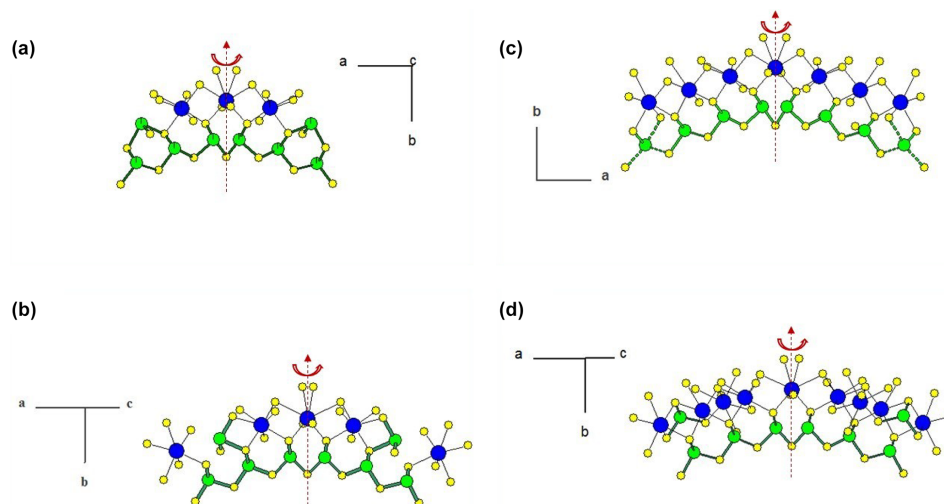


**Figure 3.** Polymerization of  $\text{SbS}_3$  polyhedra in the plagiionite series: (a) fülöppite ( $\text{Sb}_8\text{S}_{15}$ ), (b) plagiionite ( $\text{Sb}_8\text{S}_{17}$ ), (c) heteromorphite ( $\text{Sb}_8\text{S}_{19}$ ; Edenharter, 1980), and (d) semseyite ( $\text{Sb}_8\text{S}_{13}$  and two isolated  $\text{Sb}_2\text{S}_3$ ). Red: 2-fold axis.

### 3.1.3 Semseyite

Sample S1 is an old specimen from the Herja deposit (Baia Mare district, Romania). Its wet analysis (Palache et al., 1944), without minor Ag and Cu and insolubles, gave, on the basis of  $\text{Pb} + \text{Sb} = 21$  atoms per formula unit,  $\text{Pb}_{8.99}\text{Sb}_{8.01}\text{S}_{21.95}$ .

Sample S2 is centimetric massive semseyite embedded in quartz, collected in the dumps from La Rodde mine (Ally municipality, Haute-Loire department, French Massif Central; Roger, 1969). It comes from the Saint-Paul Pb-Sb quartz-baryte vein of Liassic age (Marcoux and Bril, 1986), deposited at a low temperature ( $\sim 100\text{--}150^\circ\text{C}$ ; Bril, 1982). Semseyite was the main ore mineral of this deposit.

### 3.2 Single-crystal X-ray diffraction study

Single-crystal X-ray diffraction data for the studied samples were collected using a Bruker Smart Breeze diffractometer, equipped with an air-cooled CCD detector and graphite-monochromatized  $\text{Mo } K\alpha$  radiation. The detector-to-crystal working distance was set at 50 mm. Data were corrected for Lorentz-polarization factors, absorption, and background, using the package of software APEX3 (Bruker AXS Inc., 2016). The crystal structure of plagiionite homologues was refined using SHELXL-2018 (Sheldrick, 2015), starting from the atomic coordinates given by Edenharter and Nowacki (1974), Cho and Wuensch (1974), and Matsushita (2018) for fülöppite, plagiionite, and semseyite, respectively. Scattering curves for neutral atoms were taken from the International Tables for Crystallography (Wilson, 1992). Details of data collections and refinements are given in Table 1. Atom coordinates for synthetic  $\text{Pb}_3\text{Sb}_8\text{S}_{15}$  (sample F2), plagiionite from Monte Arsiccio (sample P1), and semseyite from Herja (sample S1) are given in Table 2. Files

in Crystallographic Information File format for all the studied samples are available in the Supplement.

## 4 Crystal chemical analysis – Pb-versus-Sb substitution

### 4.1 Previous results

In the first crystal structure studies, only pure Sb and Pb sites were taken into account (see Fig. 3). During the study of a “Pb-free fülöppite”, Swinnea et al. (1985) re-examined the data of Nuffield (1975) on natural fülöppite and revealed a Pb-versus-Sb crossed substitution between neighbouring Pb(2) and Sb(3) sites, with occupancies ( $\text{Pb}_{0.825}\text{Sb}_{0.175}$ ) and ( $\text{Sb}_{0.865}\text{Pb}_{0.145}$ ), respectively. A similar result, with a weaker Pb/Sb substitution, was obtained for semseyite by Matsushita (2018) in Pb(5) and Sb(1), with occupancies ( $\text{Pb}_{0.95}\text{Sb}_{0.05}$ ) and ( $\text{Sb}_{0.95}\text{Pb}_{0.05}$ ), respectively.

### 4.2 Results from new structural studies

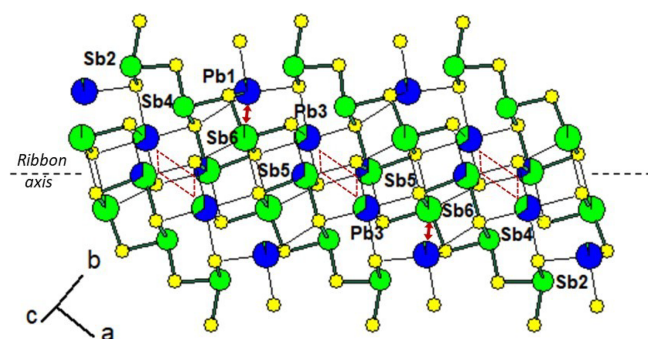
New crystal structure studies carried out on fülöppite, plagiionite, and semseyite confirm that such a Pb-versus-Sb crossed substitution is systematic in the plagiionite homologous series. Tables 3–5 summarize all measured cation site occupancy factors (SOFs), on the basis of the cation sequence defined above, together with data on mean  $\text{Me-S}$  distances and cation bond valences. In natural samples, the Pb-versus-Sb crossed substitution is the weakest in semseyite:  $x = 0.10$ , against 0.05 measured by Matsushita (2018). In plagiionite,  $x$  is close to 0.20: 0.18 (P3), 0.21 (P2), and 0.22 (P1). In natural fülöppite (F1),  $x = 0.13$ , which confirms the partitioning calculated by Swinnea et al. (1985;  $x \sim 0.16$ ) on a sample from the same ore deposit (Dealul Crucii).

Table 1. Crystal and experimental details for structure refinements of fülöppite, pligionite, and semseyite samples.

Crystal data		F1	F2	F3	P1	P2	P3	S1	S2
Crystal size (mm)		0.08 × 0.07 × 0.06	0.10 × 0.08 × 0.08	0.09 × 0.06 × 0.05	0.11 × 0.08 × 0.07	0.12 × 0.10 × 0.08	0.09 × 0.09 × 0.07	0.09 × 0.08 × 0.05	0.07 × 0.07 × 0.06
Cell setting, space group			Monoclinic, C2/c			Monoclinic, C2/c		Monoclinic, C2/c	
<i>a</i> (Å)		13.4554(8)	13.4799(6)	13.5070(11)	13.4680(14)	13.4801(5)	13.4935(5)	13.6237(5)	13.6295(4)
<i>b</i> (Å)		11.7226(7)	11.7572(5)	11.7868(10)	11.8816(13)	11.8648(4)	11.8639(4)	11.9675(4)	11.9686(3)
<i>c</i> (Å)		16.9595(10)	16.8596(8)	16.7671(14)	19.898(2)	19.9796(7)	19.9799(7)	24.5633(8)	24.5796(6)
$\beta$ (°)		94.721(3)	94.459(2)	94.746(5)	107.174(4)	107.164(2)	107.146(2)	105.9928(14)	105.996(2)
<i>V</i> (Å <sup>3</sup> )		2666.0(3)	2663.9(2)	2660.2(4)	3042.2(6)	3053.20(19)	3056.34(19)	3849.8(2)	3854.33(18)
<i>Z</i>		4	4	4	4	4	4	4	4
Data collection and refinement									
Radiation, wavelength (Å)									
Temperature (K)						MoK $\alpha$ , 0.71073			
$2\theta_{\max}$ (°)		65.10	65.17	57.14	65.14	74.41	74.35	63.04	63.10
Measured reflections		16992	22440	12097	39388	24252	23779	31049	30359
Unique reflections		4690	4838	3327	5453	7693	7218	6416	6421
Reflections with $F_o > 4\sigma(F_o)$		4095	4083	2896	5154	6414	5988	5797	5395
$R_{\text{int}}$		0.0524	0.0405	0.0494	0.0448	0.0347	0.0311	0.0593	0.0508
$R\sigma$		0.0528	0.0359	0.0461	0.0263	0.0355	0.0359	0.0451	0.0448
Range of <i>h, k, l</i>		-19 ≤ <i>h</i> ≤ 20, -17 ≤ <i>k</i> ≤ 17, -25 ≤ <i>l</i> ≤ 25	-20 ≤ <i>h</i> ≤ 16, -17 ≤ <i>k</i> ≤ 16, -25 ≤ <i>l</i> ≤ 25	-18 ≤ <i>h</i> ≤ 16, -15 ≤ <i>k</i> ≤ 15, -20 ≤ <i>l</i> ≤ 22	-20 ≤ <i>h</i> ≤ 19, -17 ≤ <i>k</i> ≤ 17, -30 ≤ <i>l</i> ≤ 30	-22 ≤ <i>h</i> ≤ 20, -19 ≤ <i>k</i> ≤ 18, -33 ≤ <i>l</i> ≤ 33	-21 ≤ <i>h</i> ≤ 22, -19 ≤ <i>k</i> ≤ 20, -33 ≤ <i>l</i> ≤ 31	-20 ≤ <i>h</i> ≤ 20, -12 ≤ <i>k</i> ≤ 17, -36 ≤ <i>l</i> ≤ 36	-15 ≤ <i>h</i> ≤ 20, -17 ≤ <i>k</i> ≤ 17, -36 ≤ <i>l</i> ≤ 36
$R [F_o > 4\sigma(F_o)]$		0.0818	0.0448	0.0562	0.0432	0.0312	0.0331	0.0399	0.0503
$R$ (all data)		0.0929	0.0570	0.0677	0.0458	0.0419	0.0449	0.0456	0.0646
$wR$ (on $F_o^2$ )		0.2044	0.0877	0.1052	0.1150	0.0724	0.0767	0.0967	0.0918
Goof		1.125	1.061	1.200	1.069	1.033	1.012	1.114	1.197
Number of least-squares parameters		129	129	129	144	144	144	181	174
Maximum and minimum residual peak ( $e \text{ \AA}^{-3}$ )		+4.54; -6.22	+4.00; -3.93	+3.21; -2.53	+4.49; -6.77	+2.69; -4.15	+4.56; -3.38	+3.60; -2.88	+2.77; -2.29

**Table 2.** Sites, site occupancy factors (SOFs), fractional atomic coordinates, and equivalent isotropic displacement parameters ( $\text{\AA}^2$ ) for selected samples of fülöppite, plagiionite, and semseyite.

Fülöppite (sample F2)					
Site	SOF	$x/a$	$y/b$	$z/c$	$U_{\text{eq}}$
Pb1	Pb <sub>0.96</sub> Sb <sub>0.04</sub>	0	0.36746(5)	1/4	0.03196(12)
Sb2	Sb <sub>1.00</sub>	0.40876(3)	0.17797(4)	0.15488(3)	0.01638(10)
Pb3a	Pb <sub>0.649</sub> (3)	0.30700(10)	0.42714(12)	0.33064(6)	0.02342(18)
Sb3b	Sb <sub>0.351</sub> (3)	0.3027(4)	0.4382(5)	0.3469(2)	0.02342(18)
Sb4	Sb <sub>1.00</sub>	0.14034(3)	0.24805(4)	0.06107(3)	0.01593(10)
Sb5a	Sb <sub>0.649</sub> (3)	0.0855(2)	0.0508(2)	0.41787(16)	0.0230(3)
Pb5b	Pb <sub>0.351</sub> (3)	0.1002(2)	0.0331(3)	0.40332(17)	0.0230(3)
Sb6a	Sb <sub>0.98</sub>	0.37403(4)	0.14016(5)	0.49440(4)	0.01984(11)
Pb6b	Pb <sub>0.02</sub>	0.3761(12)	0.1311(16)	0.4625(11)	0.01984(11)
S1	S <sub>1.00</sub>	0	0.8124(2)	1/4	0.0191(5)
S2	S <sub>1.00</sub>	0.35582(15)	0.04521(17)	0.25384(12)	0.0237(4)
S3	S <sub>1.00</sub>	0.27352(13)	0.31929(16)	0.15950(11)	0.0200(4)
S4	S <sub>1.00</sub>	0.07343(14)	0.13149(16)	0.16671(11)	0.0193(3)
S5	S <sub>1.00</sub>	0.03108(12)	0.41495(14)	0.08250(10)	0.0140(3)
S6	S <sub>1.00</sub>	0.18693(14)	0.24920(18)	0.39421(13)	0.0252(4)
S7	S <sub>1.00</sub>	0.26538(13)	0.02814(16)	0.03616(11)	0.0174(3)
S8	S <sub>1.00</sub>	0.46447(14)	0.36433(16)	0.46126(11)	0.0198(3)
Plagiionite (sample P1)					
Site	SOF	$x/a$	$y/b$	$z/c$	$U_{\text{eq}}$
Pb1	Pb <sub>1.00</sub>	1/2	0.68015(4)	3/4	0.02463(11)
Sb2	Sb <sub>1.00</sub>	0.95353(4)	0.12486(4)	0.33278(3)	0.01288(10)
Pb3	Pb <sub>1.00</sub>	-0.23144(3)	0.62603(3)	0.67762(2)	0.02006(9)
Sb4	Sb <sub>1.00</sub>	0.72928(4)	0.19067(5)	0.41358(3)	0.01263(10)
Sb5a	Sb <sub>0.780</sub> (2)	-0.00297(9)	0.51811(9)	0.60165(6)	0.01594(16)
Pb5b	Pb <sub>0.220</sub> (2)	0.02199(19)	0.5215(2)	0.62098(12)	0.01594(16)
Sb6	Sb <sub>1.00</sub>	0.49108(4)	0.30343(5)	0.47122(3)	0.01427(11)
Pb7a	Pb <sub>0.780</sub> (2)	0.26530(5)	0.41394(7)	0.55306(3)	0.01829(13)
Sb7b	Sb <sub>0.220</sub> (2)	0.2496(5)	0.4158(6)	0.5389(3)	0.01829(13)
S1	S <sub>1.00</sub>	0	0.7417(2)	3/4	0.0151(5)
S2	S <sub>1.00</sub>	0.85396(17)	-0.00507(19)	0.24478(10)	0.0179(4)
S3	S <sub>1.00</sub>	-0.81852(16)	0.73283(17)	0.66963(10)	0.0154(3)
S4	S <sub>1.00</sub>	0.61266(16)	0.07925(17)	0.32122(10)	0.0155(3)
S5	S <sub>1.00</sub>	-0.61168(15)	0.64094(15)	0.60198(9)	0.0110(3)
S6	S <sub>1.00</sub>	0.37992(16)	0.19235(18)	0.37453(11)	0.0178(4)
S7	S <sub>1.00</sub>	-0.36994(15)	0.52659(16)	0.55897(10)	0.0138(3)
S8	S <sub>1.00</sub>	0.13171(16)	0.31104(17)	0.43646(10)	0.0150(3)
S9	S <sub>1.00</sub>	-0.10741(15)	0.41579(16)	0.49835(9)	0.0130(3)
Semseyite (sample S1)					
Site	SOF	$x/a$	$y/b$	$z/c$	$U_{\text{eq}}$
Pb1	Pb <sub>1.00</sub>	0	0.70588(5)	1/4	0.02549(12)
Sb2	Sb <sub>1.00</sub>	-0.38666(4)	0.50921(5)	0.31589(2)	0.01405(11)
Pb3	Pb <sub>1.00</sub>	0.32943(3)	0.76436(3)	0.30689(2)	0.01722(8)
Sb4	Sb <sub>1.00</sub>	-0.09401(4)	0.57356(5)	0.37922(2)	0.01294(11)
Pb5	Pb <sub>1.00</sub>	0.13010(3)	0.36535(3)	0.35752(2)	0.01785(8)
Sb6	Sb <sub>1.00</sub>	0.19113(4)	0.69280(5)	0.42517(2)	0.01381(11)
Pb7	Pb <sub>1.00</sub>	0.42569(3)	0.47772(3)	0.40736(2)	0.01809(8)
Pb8a	Pb <sub>0.904</sub> (3)	0.51773(9)	0.19649(5)	0.51784(5)	0.01616(14)
Sb8b	Sb <sub>0.096</sub> (3)	0.5184(18)	0.2161(14)	0.5178(10)	0.01616(14)
Sb9a	Sb <sub>0.904</sub> (3)	0.28285(10)	0.41729(11)	0.52466(5)	0.01385(18)
Pb9b	Pb <sub>0.096</sub> (3)	0.2822(7)	0.4150(7)	0.5369(3)	0.01385(18)
S1	S <sub>1.00</sub>	-1/2	0.6458(3)	1/4	0.0164(5)
S2	S <sub>1.00</sub>	0.13859(18)	0.8837(2)	0.24384(9)	0.0184(4)
S3	S <sub>1.00</sub>	-0.25453(16)	0.65195(18)	0.31676(9)	0.0156(4)
S4	S <sub>1.00</sub>	0.44125(16)	0.97020(17)	0.30295(9)	0.0143(4)
S5	S <sub>1.00</sub>	0.00853(16)	0.74550(17)	0.36976(9)	0.0128(4)
S6	S <sub>1.00</sub>	0.22101(17)	0.58580(17)	0.34726(9)	0.0152(4)
S7	S <sub>1.00</sub>	0.71682(17)	0.13570(18)	0.59828(9)	0.0151(4)
S8	S <sub>1.00</sub>	0.48018(17)	0.30796(17)	0.60216(9)	0.0147(4)
S9	S <sub>1.00</sub>	0.10951(16)	0.47261(17)	0.45544(9)	0.0142(4)
S10	S <sub>1.00</sub>	0.32127(16)	0.29988(17)	0.45187(8)	0.0132(4)
S11	S <sub>1.00</sub>	0.38514(16)	0.57888(17)	0.50147(9)	0.0142(4)



**Figure 4.** Mixed Pb/Sb sites in the ribbon of the structure of fülöppite (sample F2 – see Table 3). Red lozenge: neighbouring (Pb,Sb)3 ( $\times 2$ ) and (Sb,Pb)5 ( $\times 2$ ) strongly mixed sites. Red arrow: (Sb,Pb)6 and (Pb,Sb)1 weakly mixed sites. For clarity, mixed sites are unsplit.

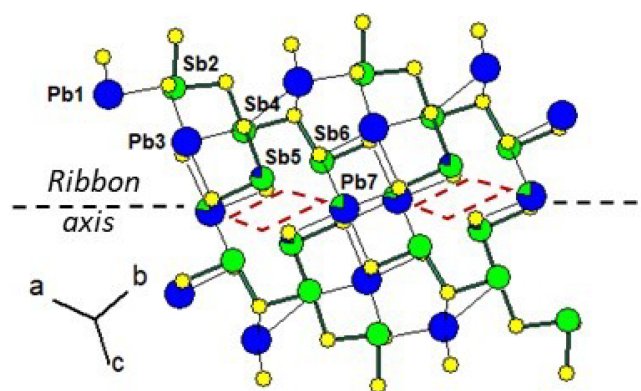
In synthetic fülöppite, the Pb/Sb substitution is very pronounced, up to  $\sim 40$  at.%. In all fülöppite samples, the refinement also reveals an Sb substitution in a Pb1 site, correlated to a Pb substitution in the two neighbouring Sb6 sites (connected to Pb1 site via two S5 sites). Although very weak in natural fülöppite ( $x' = 0.02$  in Pb1), this substitution is more pronounced in synthetic samples ( $x' = 0.04$  for F2, 0.10 for F3). It corresponds to a secondary crossed substitution:  $[\text{Pb}1_{(1-x')}\text{Sb}1_{x'}][\text{Sb}6_{(1-0.5x')}\text{Pb}6_{(1+0.5x')}]_2$ . Figure 4 represents the cation distribution within a ribbon for synthetic  $\text{Pb}_3\text{Sb}_8\text{S}_{15}$  (sample F2). While weakly mixed (Pb,Sb)1 and (Sb,Pb)6 form isolated pairs, two (Pb,Sb)3 and two (Sb,Pb)5 strongly mixed sites form a lozenge, separated from neighbouring lozenges by two Sb6 sites.

Figure 5 shows the cation distribution for pligionite from Monte Arsiccio (sample P1). Here lozenges with pairs of mixed (Pb,Sb)7 and (Sb,Pb)5 sites form a continuous file along the ribbon axis. In semseyite, lozenges with pairs of mixed (Pb,Sb)8 and (Sb,Pb)9 sites are separated by two Pb7 sites (Fig. 6), which play the same role as the Sb6 pair in fülöppite.

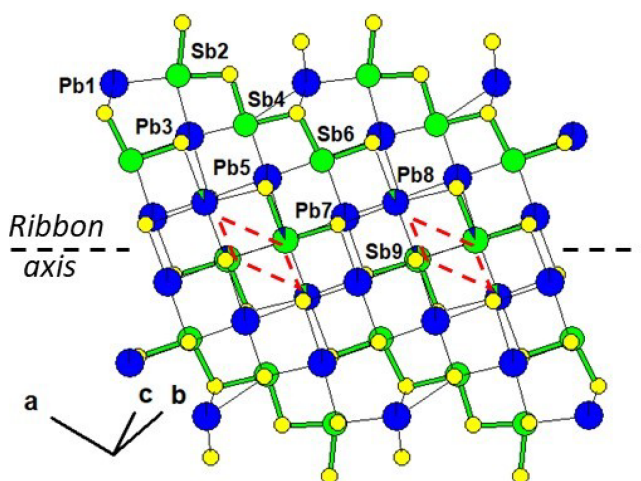
### 4.3 Relationship with unit-cell data

Table 6 compares unit-cell parameters for pligionite and semseyite. In semseyite, unit-cell data are very homogeneous. In pligionite, the unit cell measured for the sample P2 from Wolfsberg is very close to that measured by Cho and Wuensch (1974) on a crystal from the same deposit. Unit cells of samples P3 from Lepuix and P1 from Monte Arsiccio are also similar.

The three natural samples of fülöppite have very close unit-cell parameters (Table 7). They come from the same ore deposit of Dealul Crucii. Nevertheless, taking into account the two synthetic samples, there is a significant increase in  $a$  and  $b$  intra-layer parameters ( $\sim 0.5\%$ ) with an increasing Pb/Sb crossed-substitution coefficient  $x$ , while the layer stacking ( $c \cdot \sin \beta$ ) is shortened ( $\sim 1\%$  – Table 7). It corre-



**Figure 5.** Mixed Pb/Sb sites in the ribbon of the structure of pligionite from Monte Arsiccio (sample P1). Red lozenge: neighbouring (Sb,Pb)5 ( $\times 2$ ) and (Pb,Sb)7 ( $\times 2$ ) mixed sites. For clarity, mixed sites are unsplit.



**Figure 6.** Mixed Pb/Sb sites in the ribbon of the structure of semseyite from Herja (sample S1). Red lozenge: neighbouring (Pb,Sb)8 ( $\times 2$ ) and (Sb,Pb)9 ( $\times 2$ ) mixed sites. For clarity, mixed sites are unsplit.

sponds to a flattening of the unit cell along  $c$  indicated by the increase in the ratio  $(a \cdot b)/(c \cdot \sin \beta)$  (about 2% from F1 to F3). Thus, the measure of this ratio is a way to estimate the crossed-substitution coefficient  $x$ . Selecting the new data obtained with the same apparatus (F1, F2, and F3), there is also a slight decrease in the unit-cell volume.

Figure 7 compares the lozenge geometry of the  $[(\text{Pb,Sb})_3]_2[(\text{Sb,Pb})_5]_2$  groups in fülöppite (sample F2), considering the main and minor substitutions, i.e.  $(\text{Pb}_3)_2(\text{Sb}_5)_2$  and  $(\text{Sb}_3)_2(\text{Pb}_5)_2$ , respectively. The minor lozenge is compressed along  $c$  relatively to the major lozenge, as indicated by the values of their angles and diagonal lengths. Clearly, this distortion is the crystal chemical factor that controls the unit-cell flattening with an increasing  $x$  coefficient. For steric reasons, it is possible that a given layer contains

**Table 3.** Pb-versus-Sb distribution (SOF), average bond distances  $\langle Me-S \rangle$ , and cation bond valences (BVs) in the studied samples of fülöppite. For the sake of comparison, cation distribution in fülöppite from Baia Mare (Edenharter and Nowacki, 1974) and synthetic Na derivative of fülöppite (Swinnea et al., 1985) are shown.

Sample	Cation	Pb1	Sb2	Pb3a/Sb3b	Sb4	Sb5a/Pb5b	Sb6a/Pb6b
F1	Pb SOF	0.98	0	0.867	0	0.133	0.01
	Sb SOF	0.02	1	0.133	1	0.867	0.99
	$\langle Me-S \rangle$	3.195	2.470	3.012/3.031	2.490	2.569/3.054	2.524/2.912
	BV	1.95	3.05	2.19/2.37	3.11	2.78/2.44	2.95/2.77
F2	Pb SOF	0.96	0	0.649	0	0.351	0.02
	Sb SOF	0.04	1	0.351	1	0.649	0.98
	$\langle Me-S \rangle^a$	3.183	2.470	2.993/3.002	2.487	2.605/3.072	2.547/2.928
	BV	1.94	3.05	2.33/2.29	3.12	2.65/2.32	2.82/2.25
F3	Pb SOF	0.90	0	0.594	0	0.406	0.05
	Sb SOF	0.10	1	0.406	1	0.594	0.95
	$\langle Me-S \rangle$	3.178	2.468	2.991/2.997	2.487	2.611/3.075	2.552/2.925
	BV	1.90	3.06	2.36/2.26	3.13	2.61/2.31	2.79/2.27
Baia Mare	Pb SOF	1	0.825	0	0	0	0.145
	Sb SOF	0	0.175	1	1	1	0.865
Synth. Na-fül <sup>b</sup>	Pb SOF	1	0.60	0	0	0	0.40
	Sb SOF	0	0.40	1	1	1	0.60

Note that in Sb sites having Sb > 0.55 apfu, average  $\langle Me-S \rangle$  was calculated taking into account Sb-S distances shorter than 2.80 Å.

<sup>a</sup> Average distances (Å) for the three (Sb) and six (Pb) shortest bonds. <sup>b</sup> Pb derivation, according to  $Na^+ + Sb^{3+} = 2Pb^{2+}$ .

**Table 4.** Pb-versus-Sb distribution (SOF), average bond distances  $\langle Me-S \rangle$ , and cation bond valences (BVs) in the studied samples of pligionite.

Sample	Cation	Pb1	Sb2	Pb3	Sb4	Sb5a/Pb5b	Sb6	Sb7a/Pb7b
P1 Monte Arsiccio	Pb SOF	1	0	1	0	0.22	0	0.78
	Sb SOF	0	1	0	1	0.78	1	0.22
	$\langle Me-S \rangle^*$	3.038	2.463	2.968	2.476	2.587	2.523	2.982
	BV	1.87	3.09	2.16	3.23	2.67 (2.78)	2.95	2.00 (2.22)
P2 Wolfsberg	Pb SOF	1	0	1	0	0.21	0	0.79
	Sb SOF	0	1	0	1	0.79	1	0.21
	$\langle Me-S \rangle$	3.042	2.466	2.976	2.485	2.582	2.517	2.980
	BV	1.87	3.06	2.11	3.16	2.71 (2.82)	2.97	2.03 (2.18)
P3 Lepuix	Pb SOF	1	0	1	0	0.18	0	0.82
	Sb SOF	0	1	0	1	0.82	1	0.18
	$\langle Me-S \rangle$	3.040	2.468	2.975	2.486	2.588	2.521	2.980
	BV	1.87	3.05	2.12	3.15	2.67 (2.79)	2.94	2.03 (2.21)

\* Average distances (Å) for the three (Sb) and six (Pb) shortest bonds.

only one type of lozenge, i.e. exclusively  $(Pb_3)_2(Sb_5)_2$  or  $(Sb_3)_2(Pb_5)_2$  groups. The resulting crystal structure would thus correspond to a disordered interstratification of these two types of layer.

Another way to measure  $x$  is to compare the calculated XRPD of the three fülöppite samples of the present study, to see if there are some significant changes in the relative intensities of some main diffractions. On the basis of 100 for the intensity  $I$  of the  $1\bar{1}4$  reflection at 3.87 Å, there is

a significant  $I$  decrease for  $\bar{1}12$  and  $\bar{3}31$  reflections and, inversely, a significant  $I$  increase for 130 and  $\bar{2}25$  reflections (Table 8). Figure 8 represents the variation in the ratios  $A/B = I(\bar{1}12)/I(130)$  and  $C/D = I(\bar{3}31)/I(\bar{2}25)$  with  $x$  according to this table. The two continuous lines represent the interpolated curves between measured values of  $A/B$  and  $C/D$  ratios, while the two tie lines correspond to the extrapolated curves obtained starting from the crystal structure of the F1 sample, with  $x$  varying from 0 to 0.50.

**Table 5.** Lead-versus-Sb distribution (SOF), average bond distances ( $\langle Me-S \rangle$ ), and cation bond valences (BVs) in the studied samples of semseyite. For the sake of comparison, cation distribution of semseyite from Wolfsberg after Matsushita (2018) is shown.

Sample	Cation	Pb1	2 Sb2	2 Pb3	2 Sb4	2 Pb5	2 Sb6	2 Pb7	2 (Pb,Sb)8	2 (Sb,Pb)9
S1 – Herja	Pb SOF	1	0	1	0	1	0	1	0.904	0.096
	Sb SOF	0	1	0	1	0	1	0	0.096	0.904
	$\langle Me-S \rangle^*$	3.041	2.468	2.989	2.473	2.978	2.515	2.985	3.004	2.522
	BV	1.89	3.08	2.04	3.16	2.06	2.98	1.97	2.15 (2.10)	2.90 (2.90)
S2 – La Rodde	Pb SOF	1	0	1	0	1	0	1	0.926	0.074
	Sb SOF	0	1	0	1	0	1	0	0.074	0.926
	$\langle Me-S \rangle$	3.041	2.469	2.991	2.474	2.978	2.515	2.986	3.006	2.531
	BV	1.97	3.07	2.03	3.16	2.05	2.93	1.97	2.13	2.93
		Pb1	Sb4	Pb2	Sb3	Pb4	Sb2	Pb3	Pb5	Sb1
Wolfsberg	Pb SOF	1	0	1	0	1	0	1	0.922	0.046
	Sb SOF	0	1	0	1	0	1	0	0.078	0.954
	$\langle Me-S \rangle$	3.042	2.472	2.991	2.471	2.977	2.515	2.987	3.008	2.534
	BV	1.89	3.05	2.03	3.18	2.05	2.93	1.96	2.12	2.91

\* Average distances (Å) for the three (Sb) and six (Pb) shortest bonds.

**Table 6.** Relationships between unit-cell geometry and Pb/Sb crossed-substitution coefficient  $x$  in pligionite and semseyite. Samples classified according to increasing  $(a \cdot b)/(c \cdot \sin \beta)$  ratio.

(a) Semseyite									
Sample	$a$ (Å)	$b$ (Å)	$c$ (Å)	$\beta$ (°)	$V$ (Å <sup>3</sup> )	$a \cdot b$	$c \cdot \sin \beta$	$x$	$(a \cdot b)/(c \cdot \sin \beta)$
M <sup>1</sup>	13.627	11.974	24.589	105.997	3856.8	163.17	23.64	0.05	6.902
S2	13.630	11.969	24.580	105.996	3854.7	163.14	23.63	0.07	6.904
S1	13.624	11.968	24.563	105.992	3849.8	163.05	23.61	0.10	6.906
KW <sup>2</sup>	13.603	11.935	24.452	106.046	3815.2	162.35	23.50	n.d.	6.909
(b) Pligionite									
Sample	$a$ (Å)	$b$ (Å)	$c$ (Å)	$\beta$ (°)	$V$ (Å <sup>3</sup> )	$a \cdot b$	$c \cdot \sin \beta$	$x$	$(a \cdot b)/(c \cdot \sin \beta)$
P2	13.480	11.865	19.980	107.16	3053.4	159.94	19.091	0.21	8.378
CW <sup>3</sup>	13.486	11.866	19.983	107.17	3055.2	160.02	19.092	n.d.	8.381
P3	13.494	11.864	19.980	107.15	3056.4	160.09	19.092	0.18	8.385
P1	13.468	11.882	19.898	107.17	3042.3	160.03	19.011	0.22	8.418

<sup>1</sup> Matsushita (2018). <sup>2</sup> Kohatsu and Wuensch (1974b). <sup>3</sup> Cho and Wuensch (1974).

The tie line relative to the ratio  $C/D$  is in good accordance with the interpolated curve, while the  $A/B$  tie line presents a significant shift relative to the interpolated curve. The best equations are the two straight lines established on the basis of the  $A/B$  and  $C/D$  values of F1 and F2: (1)  $A/B = -0.0234x + 1.852$  and (2)  $C/D = -0.0074x + 1.307$ .

In semseyite, like in fülöppite, with increasing  $x$  the unit-cell volume decreases, while  $(a \cdot b)/(c \cdot \sin \beta)$  increases. In pligionite (Table 6b),  $x$  values are very close, which does not permit the relationships between the variations in  $x$ , unit-cell volume, and  $(a \cdot b)/(c \cdot \sin \beta)$  to be established.

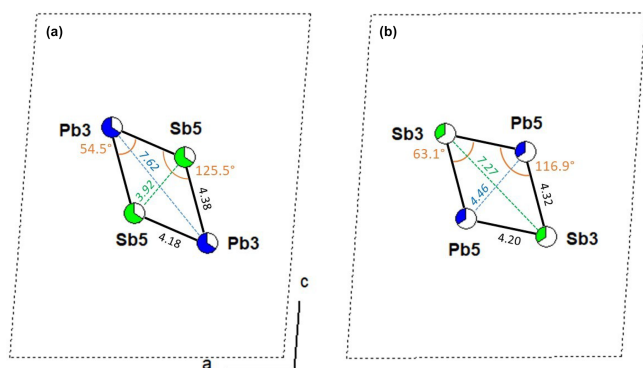
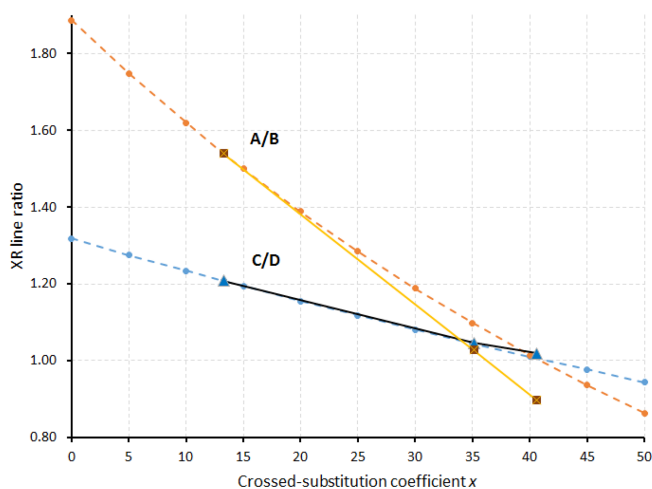
## 5 The case of Pb-free fülöppite

Swinnea et al. (1985) synthesized a Pb-free fülöppite at 250 °C in a saturated Na<sub>2</sub>CO<sub>3</sub> solution, with an ideal formula Sb<sub>10</sub>S<sub>15</sub>, implying the occurrence of vacancy ( $\square$ ) in several Sb positions. The proposed structural formula is (Sb<sub>0.58</sub> $\square$ <sub>0.42</sub>)(Sb<sub>0.852</sub> $\square$ <sub>0.148</sub>)<sub>2</sub>(Sb<sub>0.773</sub> $\square$ <sub>0.227</sub>)<sub>2</sub>Sb<sub>6</sub>S<sub>15</sub>, corresponding to Sb<sub>9.83</sub>S<sub>15</sub>, ideally Sb<sub>10</sub>S<sub>15</sub> (it would be a stibnite dimorph). Re-examination of structural data as well as synthesis conditions brings one of us (Moëlo, unpublished data) to consider this compound a Na derivative of fülöppite (briefly mentioned in Makovicky, 1989). On the one hand, this compound was obtained in a hydrothermal synthesis with a high Na concentration; on the other hand, bond-

**Table 7.** Relationships between unit-cell geometry and Pb/Sb crossed-substitution coefficient  $x$  in fülöppite. Samples classified according to increasing  $(a \cdot b)/(c \cdot \sin\beta)$  ratio.

Sample	$a$ (Å)	$b$ (Å)	$c$ (Å)	$\beta$ (°)	$V$ (Å <sup>3</sup> )	$a \cdot b$	$c \cdot \sin\beta$	$x$	$(a \cdot b)/c \cdot \sin\beta$
F1	13.4554	11.7226	16.9595	94.721	2666.0	157.73	16.902	0.14	9.332
EN <sup>a</sup>	13.435	11.727	16.934	94.70	2659.0	157.55	16.877	n.d.	9.335
N <sup>b</sup>	13.441	11.726	16.930	94.71	2659.3	157.61	16.873	0.16 <sup>c</sup>	9.341
F2	13.4799	11.7572	16.8596	94.459	2663.9	158.49	16.809	0.35	9.429
F3	13.5070	11.7868	16.7671	94.746	2660.2	159.20	16.710	0.41	9.527
Na-fül <sup>c</sup>	13.393	11.7170	16.737	93.763	2620.8	156.93	16.701	0.40 <sup>d</sup>	9.396

<sup>a</sup> Edenharter and Nowacki (1974). <sup>b</sup> Nuffield (1975). <sup>c</sup> Na-fülöppite; Swinnea et al. (1985). <sup>d</sup> Pb derivation.

**Figure 7.** Comparison of lozenge geometry of the  $[(\text{Pb,Sb})_3]_2[(\text{Sb,Pb})_5]_2$  groups with the main and minor substitutions (**a** and **b**, respectively) in fülöppite (sample F2).**Figure 8.** Variation in the  $A/B$  and  $C/D$  ratios as a function of the crossed-substitution coefficient  $x$ . Yellow line: interpolation on the basis of  $A/B$  ratios of Table 8 (brown squares); black line: interpolation on the basis of  $C/D$  ratios of Table 8 (blue triangles). Orange and blue tie lines: extrapolations of  $A/B$  and  $C/D$  ratios, respectively, on the basis of F1 crystal structure (lowest  $x$  value) as starting point for calculations.**Table 8.** Calculated relative intensities of selected  $hkl$  lines in the XRPD of fülöppite as a function of the Pb/Sb crossed-substitution coefficient  $x$ .

$hkl \rightarrow$	$\bar{1}12$		130	$\bar{3}\bar{3}1$	$\bar{2}25$		
	$x$	$A$	$B$	$C$	$D$	$A/B$	$C/D$
F1	13.3	57.1	37.1	76.3	63.2	1.540	1.208
F2	35.1	47.5	46.2	68.9	65.9	1.028	1.046
F3	40.6	43.0	47.9	67.4	66.1	0.897	1.020

$A$ ,  $B$ ,  $C$ , and  $D$ : calculated relative intensities of  $hkl$  lines.

valence calculations give bad valence sums in partially occupied Sb positions. In ideal fülöppite,  $\text{Pb}_3\text{Sb}_8\text{S}_{15}$ , the replacement of Pb through the heterovalent substitution  $2\text{Pb}^{2+} = \text{Na}^+ + \text{Sb}^{3+}$  would give the formula  $(\text{Na}_{0.5}\text{Sb}_{0.5})_3\text{Sb}_8\text{S}_{15}$ , i.e.  $\text{Na}_{1.5}\text{Sb}_{9.5}\text{S}_{15}$ .

In Pb-free fülöppite, the position Sb6 has a SOF = 0.58, corresponding to 29.6 electrons ( $e^-$ ). A mixed site with 0.5 Na and 0.5 Sb corresponds to  $(11 \times 0.5) + (51 \times 0.5) = 31 e^-$ , in quite good agreement with the measured electron density. For Sb3 (SOF = 0.852) and Sb5 (SOF = 0.773), one obtains a total of  $82.9 e^-$ . This ought to correspond to a mixture of 0.5 Na and 1.5 Sb, that is, a total of  $(11 \times 0.5) + (51 \times 1.5) = 82 e^-$ . Here also the agreement is very good. Calculation of the partitioning of Na and Sb between Sb3 and Sb5 positions gives the site populations  $(\text{Sb}_{0.81}\text{Na}_{0.19})$  and  $(\text{Sb}_{0.71}\text{Na}_{0.29})$  for Sb3 and Sb5, respectively. The developed ideal structural formula becomes  $(\text{Na}_{0.5}\text{Sb}_{0.5})(\text{Na}_{0.2}\text{Sb}_{0.8})_2(\text{Na}_{0.3}\text{Sb}_{0.7})_2\text{Sb}_6\text{S}_{15} = \text{Na}_{1.5}\text{Sb}_{9.5}\text{S}_{15}$ , as proposed above. This new structural model is shown in Fig. 8. For this structure model, bond-valence calculation according to Brese and O'Keeffe (1991) gives for the cations (1.5 Na + 9.5 Sb) a total of 29.4 vu (valence units), against 27.9 vu for the structure solution of Swinnea et al. (1985; ideal total 30 vu).

For comparison with fülöppite, the derivation of the formula of Na-fülöppite through the substitution  $\text{Na}^+ + \text{Sb}^{3+} = 2 \text{Pb}^{2+}$  gives the new formula  $\text{Pb}(\text{Sb}_{0.6}\text{Pb}_{0.4})_2(\text{Pb}_{0.6}\text{Sb}_{0.4})_2\text{Sb}_6\text{S}_{15}$ , which is very similar

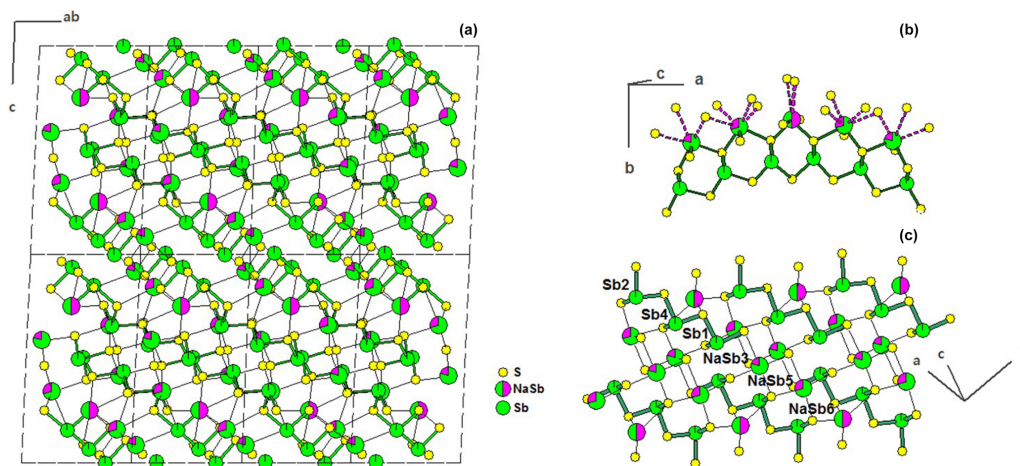


**Figure 9.** Proposed distribution of Na/Sb mixed sites in the structure of Pb-free fülöppite of Swinnea et al. (1985). (a) Projection along [110]. (b) Polymerization of cations according to short  $Me-S$  bonds. (c) Organization of the SnS-type ribbon. Pink sectors: Na fraction in mixed (Sb, Na) positions.

to the formula of the synthetic fülöppite studied in this work (sample F3). It corresponds to the row sequence Sb–Sb–Sb–(Pb<sub>0.6</sub>Sb<sub>0.4</sub>)–(Sb<sub>0.6</sub>Pb<sub>0.4</sub>)–Pb (Table 3).

The actual formula of Pb-free fülöppite appears to be Na<sub>1.5</sub>Sb<sub>9.5</sub>S<sub>15</sub> (or Na<sub>3</sub>Sb<sub>19</sub>S<sub>30</sub>). It is a new Na-poor member of the pseudo-binary Na<sub>2</sub>S–Sb<sub>2</sub>S<sub>3</sub> system, together with NaSbS<sub>2</sub> (a dimorph pair; Olivier-Fourcade et al., 1978) and Na<sub>3</sub>SbS<sub>3</sub> (Sommer and Hope, 1977; Pompe and Pfitzner, 2013).

Mozgova et al. (1987) detected the presence of hydrogen as (HS)<sup>–</sup> or (OH)<sup>–</sup> in synthetic fülöppite through NMR study. Due to the synthesis conditions (pH ~ 1.5), it is probable that H<sup>+</sup> substitutes in the crystal structure in a similar way to Na<sup>+</sup>, i.e. in the sense that 2Pb<sup>2+</sup> = H<sup>+</sup> + Sb<sup>3+</sup>.

## 6 Discussion and conclusion

These new crystal structure refinements confirm that the Pb-versus-Sb crossed substitutions in two neighbouring metal positions in the middle of the constitutive layers are a systematic feature for fülöppite, pligionite, and semseyite, and this ought to be confirmed for the fourth member heteromorphite. The developed structural formula of this homologous series can be given as Pb<sub>2N–1</sub>(Pb<sub>1–x</sub>Sb<sub>x</sub>)<sub>2</sub>(Sb<sub>1–x</sub>Pb<sub>x</sub>)<sub>2</sub>Sb<sub>6</sub>S<sub>13+2N</sub>. This substitution is isochemical, as it does not change the composition of the compound. Its level is very variable, according to the species (lowest percentages in the Pb-richest member semseyite) or in a given species (fülöppite  $x \sim 0.10$  at. % to 0.40 at. %). Such a crossed substitution corresponds to a competition between two sequences in the cation rows distinguished in the structures, (Sb–Sb–Sb)–Pb–Sb(…), major in pligionite, semseyite, and the calculated Pb derivative of Na-fülöppite, on the one hand, and, on the other hand,

(Sb–Sb–Sb)–Sb–Pb(…), major in fülöppite and probably also in heteromorphite. It is likely that this crossed substitution could attenuate steric distortions in the middle of the SnS-type layers of the pligionite homologous series, in relationship to the layer flattening evidenced in fülöppite.

At present, it is difficult to clearly understand which physicochemical factors control this substitution. If such a disorder was related to temperature ( $T$ ), the substitution would increase accordingly. However, the substitution coefficient  $x$  is lower in the synthetic F2 sample (obtained at 270–300 °C) than in the synthetic F3 sample (obtained at 200 °C). A pressure increase would favour the volume decrease observed in fülöppite. However, this is not apparently in accordance with experiments, as, in hydrothermal conditions, the pressure at the equilibrium H<sub>2</sub>O<sub>liqu.</sub> ↔ H<sub>2</sub>O<sub>vap.</sub>, increasing with  $T$ , corresponds to a lower, and not higher,  $x$  value from the F3 sample (200 °C) compared to F2 (270–300 °C). The kinetics of crystallization may play a crucial role, as the substitution coefficient  $x$  is the highest in synthetic samples, which are obtained rapidly compared to natural growth conditions in ore deposits.

According to thermodynamic principles, in normal conditions, samples with different  $x$  coefficients cannot correspond to identical energy levels. It is probable that natural fülöppite samples, grown closer to equilibrium conditions, correspond to the more stable composition (lowest  $x$  value), where (Pb<sub>3</sub>)<sub>2</sub>(Sb<sub>5</sub>)<sub>2</sub> prevails over (Sb<sub>3</sub>)<sub>2</sub>(Pb<sub>5</sub>)<sub>2</sub>.

Systematic but variable Pb-versus-Sb crossed substitution in a cation pair, without change in the chemical composition, is an original crystal chemical feature of the pligionite series. Resolution of new crystal structures among different members of the series, especially synthetic ones, will help in the understanding of what physical factors control fluctuations in such a crossed substitution. It is also possible that well-

resolved structures will reveal modulations due to long-range ordering along *c* of two types of layers, as suggested here for fülöppite. The use of transmission electron microscopy (HRTEM) may be decisive for this purpose.

Recently, a similar crossed substitution implying two neighbouring (Pb, As) mixed sites has been observed in tsugaruite,  $\text{Pb}_{28}\text{As}_{15}\text{S}_{50}\text{Cl}$  (Biagioni et al., 2020). These two sites have  $\text{As}_{0.65}\text{Pb}_{0.35}$  and  $\text{Pb}_{0.61}\text{As}_{0.39}$  occupations, giving the structural formula  $\text{Pb}_{26}(\text{Pb}_{0.6}\text{As}_{0.4})_2(\text{Pb}_{0.4}\text{As}_{0.6})_2\text{As}_{13}\text{S}_{50}\text{Cl}$ .

It would be interesting to synthesize Pb-free fülöppite by dry synthesis in the  $\text{Na}_2\text{S-Sb}_2\text{S}_3$  system, in order to confirm and refine its structure. This would permit the characterization of its physical properties, taking into account the recent interest of parent  $\text{NaSbS}_2$  as a solar absorber material (Sun and Singh, 2017). In addition, it is possible that Na enters as traces in the structures of natural members of the pligionite series, in relationship to the NaCl concentration of hydrothermal solutions. Similarly, NMR study of hydrogen as traces may help to measure the pH of these solutions.

*Data availability.* Crystallographic Information Files (CIFs) of the studied crystal structures are available in the Supplement.

*Supplement.* The supplement related to this article is available online at: <https://doi.org/10.5194/ejm-32-623-2020-supplement>.

*Author contributions.* CB carried out the single-crystal data collection. Both the authors analysed the results and wrote the manuscript.

*Competing interests.* The authors declare that they have no conflict of interest.

*Acknowledgements.* Crystals of synthetic fülöppite were kindly given to one of us (Yves Moëlo) by Nadejda Mozgova (IGEM Moscow), to whom this study is devoted. We sincerely thank Cristiana L. Ciobanu (University of Adelaide) and Emil Makovicky for their careful reading of the manuscript. Federica Zaccarini (Department of Applied Geosciences and Geophysics, University of Leoben) is sincerely thanked for her help with microprobe analysis.

*Financial support.* This research received support from the Ministero dell'Istruzione, dell'Università e della Ricerca through the project PRIN 2017 "TEOREM – deciphering geological processes using Terrestrial and Extraterrestrial ORE Minerals", prot. 2017AK8C32.

*Review statement.* This paper was edited by Giuseppe Cruciani and reviewed by Emil Makovicky and Cristiana L. Ciobanu.

## References

- Basu, K., Bortnikov, N. S., Mookherjee, A., Mozgova, N. N., Tsepina, A. I., and Vyalsov, L. N.: Rare minerals from Rajpura-Dariba, Rajasthan, India, IV: a new Pb-Ag-Tl-Sb sulphosalt, rayite, *Neues Jb. Miner. Monat.*, 1983, 296–304, 1983.
- Bente, K. and Meier-Salimi, M.: Substitution experiments and structure investigations on Ag-Tl bearing boulangerites – a contribution to the rayite problem, *Neues Jb. Miner. Abh.*, 163, 212–216, 1991.
- Biagioni, C., Bindi, L., Momma, K., Miyawaki, R., Matsushita, Y., and Moëlo, Y.: Determination of the crystal structure and redefinition of tsugaruite,  $\text{Pb}_{28}\text{As}_{15}\text{S}_{50}\text{Cl}$ , the first lead-arsenic chloro-sulfosalt, *Can. Mineral.*, in press, 2020.
- Breese, N. E. and O'Keeffe, M.: Bond-valence parameters for solids, *Acta Crystallogr.*, B47, 192–197, 1991.
- Bril, H.: Fluid inclusion study of Sn-W-Au, Sb- and Pb-Zn mineralizations from the Brioude-Massiac district (French Massif Central), *Tscher. Miner. Petrog.*, 30, 1–16, 1982.
- Bruker AXS Inc.: Apex 3. Bruker Advanced X-ray Solutions, Madison, Wisconsin, USA, 2016.
- Cho, S.-A. and Wuensch, B. J.: Crystal chemistry of the pligionite group, *Nature*, 225, 444–445, 1970.
- Cho, S.-A. and Wuensch, B. J.: The crystal structure of pligionite,  $\text{Pb}_5\text{Sb}_8\text{S}_{17}$ , the second member of the homologous series  $\text{Pb}_{3+2n}\text{Sb}_8\text{S}_{15+2n}$ , *Z. Kristallogr.*, 139, 351–378, 1974.
- Costagliola, P., Benvenuti, M., Tanelli, G., Cortecchi, G., and Lattanzi, P.: The barite-pyrite-iron oxides deposit of Monte Arsiccio (Apuane Alps), Geological setting, mineralogy, fluid inclusions, stable isotopes and genesis, *Boll. Soc. Geol. Ital.*, 109, 267–277, 1990.
- Edenharter, A.: Die Kristallstruktur von Heteromorphit,  $\text{Pb}_7\text{Sb}_8\text{S}_{19}$ , *Z. Kristallogr.*, 151, 193–202, 1980.
- Edenharter, A. and Nowacki, W.: Die Kristallstruktur von fülöppit,  $\text{Pb}_3\text{Sb}_8\text{S}_{15}$ , *Neues Jb. Miner. Monat.*, 92–94, 1974.
- Edenharter, A. and Nowacki, W.: Die Kristallstruktur von fülöppit ( $\text{Sb}_8\text{S}_{15}$ )( $\text{Pb}^{\text{VIII}}\text{Pb}_2^{\text{VI}}$ ), *Z. Kristallogr.*, 142, 196–215, 1975a.
- Edenharter, A. and Nowacki, W.: Die Kristallstruktur von Heteromorphit  $\text{Pb}_7\text{Sb}_8\text{S}_{19}$ , *Neues Jb. Miner. Monat.*, 1975, 193–195, 1975b.
- Fluck, P., Weil, R., and Wimmenauer, W.: Géologie des gîtes minéraux des Vosges et des régions limitrophes, *Mémoires du B.R.G.M. No 87*, B.R.G.M. Ed. (Orléans), 189 pp., 1975.
- Janković, S., Mozgova, N. N., and Borodaev, Yu. S.: The complex antimony-lead/zinc deposit at Rujevaca/Yugoslavia; its specific geological and mineralogical features, *Miner. Deposita*, 12, 381–392, 1977.
- Kohatsu, J. J. and Wuensch, B. J.: Semseyite ( $\text{Pb}_9\text{Sb}_8\text{S}_{21}$ ) and the crystal chemistry of the pligionite group,  $\text{Pb}_{3+2n}\text{Sb}_8\text{S}_{15+2n}$ , in: American Crystallographic Association Spring Meeting, March 1974, Selected abstracts, *Am. Mineral.*, 59, 1127, 1974a.
- Kohatsu, J. J. and Wuensch, B. J.: Prediction of structures in the homologous series  $\text{Pb}_{3+2n}\text{Sb}_8\text{S}_{15+2n}$  (the pligionite group), *Acta Crystallogr.*, 30, 2935–2937, 1974b.

- Makovicky, E.: Modular classification of sulfosalts – current status. Definition and application of homologous series, *Neues Jb. Miner. Abh.*, 160, 269–297, 1989.
- Makovicky, E.: Algorithms for calculations of homologous order  $N$  in the homologous series of sulfosalts, *Eur. J. Mineral.*, 31, 83–97, <https://doi.org/10.1127/ejm/2018/0030-2791>, 2019.
- Marcoux, E. and Bril, H.: Héritage et source des métaux d'après la géochimie isotopique du plomb. Exemple des minéralisations filoniennes (Sb, Pb, Ba, F) du Haut-Allier (Massif Central, France), *Miner. Deposita*, 21, 35–43, 1986.
- Matsushita, Y.: Re-investigation of the crystal structure of semseyite,  $\text{Pb}_9\text{Sb}_8\text{S}_{21}$ , *Z. Kristallogr.*, 233, 279–284, <https://doi.org/10.1515/zkri-2017-2108>, 2018.
- Matsushita, Y., Nishi, F., and Takéuchi, Y.: The crystal structure of semseyite,  $\text{Pb}_9\text{Sb}_8\text{S}_{21}$ , in: *Tropochemical cell-twinning. A structure building mechanism in crystalline solids*, Terra Scientific Publishing Company, Tokyo, Japan, 288–293, 1997.
- Moëlo, Y.: Quaternary compounds in the system Pb-Sb-S-Cl: Dadsonite and synthetic phases, *Can. Mineral.*, 17, 595–600, 1979.
- Moëlo, Y.: Contribution à l'étude des conditions naturelles de formation des sulfures complexes d'antimoine et plomb, *Signification métallogénique*, Document B.R.G.M., 57, B.R.G.M. Ed., Orléans, 624 pp., 1983.
- Moëlo, Y., Borodaev, Yu., and Mozgova, N. N.: Association twinnite-zinkénite-pligionite du gisement complexe à Sb-Pb-Zn de Rujevac (Yougoslavie), *B. Minéral.*, 106, 505–510, 1983.
- Mozgova, N. N. and Borodaev, Yu. S.: Homology in semseyite-fülöppite, *Zap. Vs. Mineral. Obsch.*, 3, 299–312, 1972 (in Russian).
- Mozgova, N. N., Bondar, A. M., Balitskaya, O. N., and Proshko, V. Ya.: Presence of hydrogen in sulfosalts according to nuclear magnetic resonance, *Dokl. Acad. Nauk SSSR, Mineral.*, 295, 700–702, 1987 (in Russian).
- Nuffield, E. W.: The crystal structure of fülöppite,  $\text{Pb}_3\text{Sb}_8\text{S}_{15}$ , *Acta Crystallogr.*, B31, 151–157, 1975.
- Olivier-Fourcade, J., Philippot, E., and Maurin, M.: Structure des composés  $\text{NaSbS}_2\alpha$  et  $\text{NaSbS}_2\beta$ . Etude de l'influence de la paire électronique E de l'antimoine III dans la transition  $\text{NaSbS}_2\alpha \rightarrow \text{NaSbS}_2\beta$ , *Z. Anorg. Allg. Chem.*, 446, 159–168, 1978.
- Palache, C., Berman, H., and Frondel, C.: Dana's system of mineralogy, 7th Edn., vol. I, John Wiley and Sons, 466–468, 1944.
- Pompe, C. and Pfitzner, A.:  $\text{Na}_3\text{SbS}_3$ : Single crystal X-ray diffraction, Raman spectroscopy, and impedance measurements, *Z. Anorg. Allg. Chem.*, 639, 296–300, <https://doi.org/10.1002/zaac.201200511>, 2013.
- Roger, G.: Sur la minéralogie et le mode de gisement des filons à antimoine du district de Brioude-Massiac (Haute-Loire, Cantal), *Massif Central français, B. Soc. Fr. Minéral. Cr.*, 92, 76–95, 1969.
- Rose, G.: Über die Krystallform des Pligionits, ein neues Antimonerzes, *Pogg. Ann. Phys. Chem.*, 28, 421–424, 1833.
- Roy Choudury, K., Bente, K., and Mookherjee, A.: Chemical and structural correlation problems of rayite, *Neues Jb. Miner. Abh.*, 160, 30–33, 1989.
- Sheldrick, G. M.: Crystal structure refinement with SHELXL, *Acta Crystallogr.*, C71, 3–8, <https://doi.org/10.1107/S2053229614024218>, 2015.
- Sommer, H. and Hoppe, R.: Über ternäre Sulfide der Alkalimetalle mit Arsen und Antimon, *Z. Anorg. Allg. Chem.*, 430, 199–210, 1977.
- Spencer, L. S.: Pligionite, heteromorphite and semseyite as members of a natural group of minerals, *Mineral. Mag.*, 55, 55–68, 1899.
- Sung, J. and Singh, D.J.: Electronic properties, screening and efficient carrier transport in  $\text{NaSbS}_2$ , *Phys. Rev. Appl.*, 7, 024015, <https://doi.org/10.1103/PhysRevApplied.7.024015>, 2017.
- Swinnea, J. S., Tenorio, A. J., and Steinfink, H.:  $\text{Sb}_{10}\text{S}_{15}$ , a Pb-free analog of fülöppite,  $\text{Pb}_3\text{Sb}_8\text{S}_{15}$ , *Am. Mineral.*, 70, 1056–1058, 1985.
- Takéuchi, Y.: The pligionite homologous series, in: *Tropochemical cell-twinning. A structure-building mechanism in crystalline solids*, Tokyo, Terra Scientific Publishing Company, chap. 7, 161–213, 1997.
- Weil, R., Siat, A., and Fluck, P.: Espèces inédites ou rares des Vosges, *Sci. Géol., Bull.*, Strasbourg, 28, 261–282, 1975.
- Wilson, A. J. C. (Ed.): *International Tables for Crystallography, Volume C: Mathematical, physical and chemical tables*, Kluwer Academic, Dordrecht, NL, 1992.